Applied Microbiology and Biotechnology
https://doi.org/10.1007/s00253-018-9136-9

BIOTECHNOLOGICALLY RELEVANT ENZYMES AND PROTEINS

The βγ-crystallin domain of *Lysinibacillus sphaericus* phosphatidylinositol phospholipase C plays a central role in protein stability

Sebastián Cerminati[1] · Luciana Paoletti[1] · Salvador Peirú[1] · Hugo G. Menzella[1] · María Eugenia Castelli[1]

Received: 28 December 2017 / Revised: 25 April 2018 / Accepted: 23 May 2018

Abstract

βγ-crystallin has emerged as a superfamily of structurally homologous proteins with representatives across all domains of life. A major portion of this superfamily is constituted by microbial members. This superfamily has also been recognized as a novel group of Ca^{2+}-binding proteins with a large diversity and variable properties in Ca^{2+} binding and stability. We have recently described a new phosphatidylinositol phospholipase C from *Lysinibacillus sphaericus* (LS-PIPLC) which was shown to efficiently remove phosphatidylinositol from crude vegetable oil. Here, the role of the C-terminal βγ-crystallin domain of LS-PIPLC was analyzed in the context of the whole protein. A truncated protein in which the C-terminal βγ-crystallin domain was deleted ($LS\text{-}PIPLC_{\Delta CRY}$) is catalytically as efficient as the full-length protein (LS-PIPLC). However, the thermal and chemical stability of $LS\text{-}PIPLC_{\Delta CRY}$ are highly affected, demonstrating a stabilizing role for this domain. It is also shown that the presence of Ca^{2+} increases the thermal and chemical stability of the protein both in aqueous media and in oil, making LS-PIPLC an excellent candidate for use in industrial soybean oil degumming.

Keywords Crystal domain · Phosphatidylinositol phospholipase C · Protein stability

Introduction

βγ-crystallin is a protein superfamily with diverse members present in all domains of life (Srivastava et al. 2017; Suman et al. 2013). Proteins belonging to the βγ-crystallin superfamily contain a domain formed by two Greek key motifs arranged as four-stranded antiparallel β-sheets referred to as the crystallin fold or βγ-motif (Jaenicke and Slingsby 2001; Suman et al. 2013). The βγ-crystallin domains are stable domains thought to have evolved as a result of a gene duplication event at the level of the motif. They are prevalent in a wide variety of proteins as single βγ-crystallin domains, pairs of (or multiple) domains, and domains in combination with several other domains as part of complex domain architectures (Jaenicke and Slingsby 2001; Mishra et al. 2014).

βγ-crystallins are important constituents of the vertebrate eye and most studies have been conducted focusing on their stability, genetics, and implications in cataractogenesis (Bloemendal et al. 2004; Vendra et al. 2016). There are few experimentally studied examples among bacterial members of this superfamily: Protein S from *Myxococcus xanthus* is a spore coat protein containing two βγ-crystallin domains (Teintze et al. 1988), and *Yersinia* crystallin YPO2884 is a Ca^{2+}-binding protein containing three βγ-crystallin domains (Jobby and Sharma 2005). Many bacterial βγ-crystallin-isolated domains have been studied structurally: clostrillin from *Clostridium beijerinckii*, flavollin from *Flavobacterium johnsoniae*, rhodollin from *Rhodoferax ferrireducens*, reinekllin from *Reinekea* sp., and nitrollin from *Nitrosospira multiformis* (Aravind et al. 2009a, b; Suman et al. 2013).

Microbial members of the βγ-crystallin superfamily have functional Ca^{2+}-binding sites, while most of the Ca^{2+}-binding sites of mammalian and higher vertebrate members are inactive (Mishra et al. 2014). In the configuration of βγ-

Electronic supplementary material The online version of this article (https://doi.org/10.1007/s00253-018-9136-9) contains supplementary material, which is available to authorized users.

✉ María Eugenia Castelli
castelli@iprobyq-conicet.gob.ar

[1] CONICET y Departamento de Tecnología, Facultad de Ciencias Bioquímicas y Farmacéuticas, Instituto de Procesos Biotecnológicos y Químicos (IPROBYQ), Universidad Nacional de Rosario (UNR), Suipacha 531, 2000 Rosario, Argentina

Published online: 16 June 2018

crystallins, there are two Ca^{2+}-binding sites in which the participating residues mainly belong to two N/D-N/D-X-X-S/T-S stretches of the loops connecting the third and fourth β-strands in both Greek key motifs. The two motifs coordinate Ca^{2+} ions in an interlocking fashion (Clout et al. 2001). This design gives the motif its name "double clamp motif."

The βγ-crystallins that contain the Ca^{2+}-binding motif bind Ca^{2+} with affinities in the low micromolar range and do not undergo major structural changes upon Ca^{2+} binding (Suman et al. 2011). However, the domains assume a reduced hydrodynamic size and thermodynamically drift to a state of higher structural stabilization. Therefore, in some βγ-crystallins, Ca^{2+} plays the role of an intrinsic stabilizer (Srivastava et al. 2014). Within the superfamily, there exists a stability gradient across the domains and differences in the extent of gain in stability upon Ca^{2+} binding (Kozlyuk et al. 2016; Suman et al. 2011, 2013).

Although the βγ-crystallin superfamily constitutes one of the most prevalent groups of bacterial Ca^{2+}-binding proteins, Ca^{2+} binding has only been studied with isolated βγ-crystallin domains, with the role of cation binding in multidomain proteins and the physiological role of these proteins still unknown.

While searching for thermostable enzymes to be used in the hydrolysis of phosphatidylinositol for industrial oil degumming, we have recently expressed a new phosphatidylinositol phospholipase C from *Lysinibacillus sphaericus* (LS-PIPLC) and developed a fed-batch fermentation process in *Escherichia coli* that produces ~ 14 g/l of the recombinant enzyme (Cerminati et al. 2017).

Phospholipases C hydrolyze phospholipids, generating diacylglycerol and phosphate head groups that are highly hydrophilic. Crude soybean oil contains 1.75–3% of phospholipids or "gums" that can be partially or completely removed from oil by using different methods, specifically water degumming, acid degumming, or enzymatic degumming (Erickson 1995). Enzymatic degumming by using phospholipase C enzymes is used in industry as an environmentally friendly process with an improved yield of oil recovery (Dijkstra 2011).

Most of the predicted βγ-crystallins are yet to be characterized experimentally, and previous research has been limited to structural and Ca^{2+}-binding studies of isolated domains. In this work, the function of a βγ-crystallin domain is analyzed in a multidomain bacterial secreted phospholipase, LS-PIPLC.

We report the identification of LS-PIPLC as a member of the βγ-crystallin superfamily and show that the βγ-crystallin domain of LS-PIPLC is not involved directly with the catalytic activity of the phospholipase but has a fundamental role in the thermal and chemical stability of the protein. It is also shown that the presence of Ca^{2+} increases the thermal and chemical stability of the protein both in aqueous media and in oil. The high stability of LS-PIPLC, in addition to its catalytic properties, makes this protein an excellent candidate for use in industrial soybean oil degumming.

Materials and methods

Strains and growth conditions

The *Escherichia coli* Top10 (Invitrogen) strain was used for general purposes, and *E. coli* BL21AI (Studier et al. 1990) was used to express proteins. The strains were grown in Luria Bertani (LB) medium at 200 rpm and 37 °C. The concentration of kanamycin used was 50 mg/L.

DNA preparation, cloning, and transformation of *E. coli*

Restriction enzymes, T4 ligase, and Taq polymerase were purchased from New England Biolabs. Plasmid DNA was prepared by using the Axygen Biosciences Axy-Prep™ Plasmid Minipreps Kit.

The deletion of the βγ-crystallin domain from LS-PIPLC gene was performed by PCR by using the following primers: pBAD-Fw (5′-ATGCCATAGCATTTTTATCC-3′), PIPLC$_{\Delta CRY}$*Hin*dIII Rv (5′-GAAGAGATTATCAG AGCCAACAAAAGCTTAGT-3′). Plasmid pKCN233 was used as the template (Cerminati et al. 2017). The PCR product was digested with the *Nde*I and *Hin*dIII restriction enzymes and cloned into the pKCN-His BAD plasmid digested with the same enzymes, in order to obtain plasmid pKCN241 (pKCN-His BAD::LSPIPLC$_{\Delta CRY}$).

Preparation of electrocompetent cells of *E. coli* was performed according to the protocols described by Sambrook et al. (1989). All plasmids were introduced into *E. coli* by using a BioRad Pulse Controller® apparatus according to the manufacturer's specifications.

Protein expression and purification

Protein expression and purification were performed mostly as previously reported (Cerminati et al. 2017). Briefly, *E. coli* BL21AI strains carrying the expression plasmids (pKCN233 and pKCN241) were grown overnight in LB medium. A 100-fold dilution of the cultures was made in the same medium and, when the OD 600 nm reached 0.5, the cultures were induced with 0.4 g/L of L-arabinose (Royal Cosun, Netherlands) for 6 h at 30 °C.

Subsequently, cells were collected by centrifugation, washed, and resuspended in buffer A (15 mM sodium phosphate pH 7.0, 500 mM NaCl) with 5 mM imidazole, prior to disruption by sonication in a GEX 600 Ultrasonic Processor. After the cell debris was removed by centrifugation, the

supernatants were passed through a Ni^{2+}-NTA-agarose affinity column (GE Life Sciences) equilibrated with buffer A containing 5 mM imidazole. After the columns were washed with buffer A with 20 mM imidazole, the PIPLC proteins were recovered by elution with 0.5 M imidazole and exhaustive dialysis in enzyme dilution buffer (15 mM sodium phosphate,10% glycerol, pH 7). Protein homogeneity (more than 90% pure) was analyzed by SDS-PAGE. All procedures were carried out at 4 °C.

Enzymatic activity measurements

The fluorogenic substrate butyl-fluorescein myo-inositol (B-FLIP, Toronto Research Chemicals) was used for activity assays mostly as described previously (Cerminati et al. 2017). To determine fluorescence, 200-μL aliquots of each sample, composed of 50 μL of 4× buffer assay (0.2 M sodium acetate, pH 5.5; 4 μM BSA), the indicated concentration of B-FLIP (diluted in order to use 2 μL per reaction), 10 μL of the corresponding enzyme dilution, and 138 μL of H_2O were applied in triplicate into a 96-well flat bottom black plate (Greiner Bio-One). Fluorescence was recorded by using a Synergy Multi-Mode Micro Plate Reader (Bio-Tek) with 485 ± 20- and 528 ± 20-nm filters for excitation and emission wavelengths, respectively. A 3-min time scan was first taken with all components except the enzyme. Then 10 μL of the enzyme dilutions were added and a second 3-min time scan was recorded.

The kinetic data obtained for LS-PIPLC or LS-PIPLC$_{\Delta CRY}$ were fitted to the empirical Hill equation, which in enzyme kinetics takes the following form (Wedler 1976):

$$v = \frac{V_{h\max}\,[S]^n}{K_h^n + [S]^n},$$

where $V_{h\max}$, K_h, and n are empirical parameters derived from the data, and [S] is the concentration of the substrate. The fit was performed by using GraphPad Prism 5 software.

For residual activity measurements, enzymes solutions were preincubated for 15 min at the specified temperatures before determining enzyme activity.

Thermal denaturation experiments

Thermal denaturation experiments were carried out mostly as described previously (Huynh and Partch 2015). Briefly, a real-time PCR device (Veriti) was used to monitor protein unfolding by the increase in the fluorescence of the fluorophore SYPRO Orange (Invitrogen). Five-micromolar protein samples in 150 mM NaCl and 15 mM HEPES buffer, pH 7.0, were incubated with 1× SYPRO orange (Life technologies) in PCR tubes in a final volume of 50 μL. The samples were heated at 1 °C per minute, from 25 to 95 °C. The fluorescence intensity was measured at every temperature. The data were normalized and fitted by using mostly the method previously described (Huynh and Partch 2015).

Chemical denaturation experiments

Chemical denaturation assays were performed with increasing concentrations of urea (0–8 M) or guanidinium chloride (0–6 M) in 50 mM HEPES, pH 7.0, in the presence of 1 mM EDTA or 1 mM $CaCl_2$. Samples were allowed to equilibrate for 24 h with denaturants before fluorescence spectra were acquired.

Fluorescence spectroscopy

Tryptophan fluorescence of purified proteins was measured in 50 mM HEPES, pH 7.0, in the presence of either 1 mM EDTA or 1 mM $CaCl_2$ at room temperature. Fluorescence emission spectra (300–420 nm) were acquired by using an Aminco-Bowman series 2 fluorescence spectrophotometer with 1-nm excitation slits and an excitation wavelength of 280 nm. Each spectrum was the average of three scans. The ratio of the signals at 352 nm (corresponding to solvent-exposed tryptophan) and at 336 nm (corresponding to buried tryptophan) was used to monitor protein unfolding in chemical denaturation experiments. Data were normalized and $[\text{denaturant}]_{1/2}$ was calculated as previously described (Pace et al. 1992; Santoro and Bolen 1988).

Enzymatic oil degumming and inorganic phosphate analysis

Oil degumming experiments were performed mostly as describe previously by using 3 g of crude soybean oil (Molinos Río de la Plata, Argentina) (Castelli et al. 2016; Ravasi et al. 2015). Briefly, the crude oil was preincubated at 50 °C in a VP710 stirrer (V&P Scientific Inc.) and then 90 μL of the corresponding enzyme (7.5 μM) was emulsified by using an Ultra-Turrax T 8 Homogenizer. Continuous stirring (500 rpm) was maintained at 50 °C for 2 h.

For phosphate determination, the degummed oil was homogenized with an Ultra-Turrax T8, and 200 mg of the homogenized oil was mixed with 200 μL of 1 M Tris-HCl at pH 8. Then 800 μL of water was added, and the mixture was incubated for 1 h at 37 °C with constant agitation and centrifuged for 5 min at 14000*g*. Forty-five microliters of the aqueous phase was recovered and treated with 0.3 U of calf intestinal phosphatase (Promega, WI, USA) for 1 h at 37 °C, following the manufacturer's instructions. Finally, inorganic phosphate was determined according to the method of Sumner (1944). Spectrophotometric readings were made at 700 nm in a Novaspect III apparatus (Amersham Bioscience). The micromoles of inorganic phosphate in the

samples were calculated from a standard curve containing 0.025 to 0.25 μmol of inorganic phosphate.

Results

Protein expression, purification, and biochemical characterization

LS-PIPLC is a protein with 417 amino acids (Fig. 1a). An N-terminal signal sequence consists of 40 amino acids. Two other well-defined domains exist: an N-terminal phosphatidylinositol diacylglycerol-lyase domain between amino acid residues 48–317, and a C-terminal βγ-crystallin domain between amino acid residues 328–417. Sequence alignment of the LS-PIPLC βγ-crystallin domain with other members of the superfamily shows in this domain conservation of all of the characteristic motifs, including the two Ca^{2+}-binding motifs (N/D-N/D-X-X-S/T-S fingerprint) (Fig. 1b).

In order to evaluate whether the βγ-crystallin domain present in LS-PIPLC confers stability to the entire protein, the full-length gene of LS-PIPLC and a shorter version were cloned into a vector to express the full-length protein and a truncated version that lacked the C-terminal βγ-crystallin domain, respectively [PI-PLC$_{\Delta CRY}$ containing only the PIPLC domain (Fig. 1c), see "Materials and methods"].

LS-PIPLC and LS-PIPLC$_{\Delta CRY}$ were purified as His-tag fusion proteins with molecular weights of 45.16 and 34.66 kDa, respectively (see "Materials and methods"). Next, the enzymatic PIPLC activity was assayed by using the water-soluble fluorogenic substrate butyl-fluorescein myo-inositol phosphate (B-FLIP), as previously described (Cerminati et al. 2017). The parameters obtained from a non-linear regression fit of the data of Fig. 2 are summarized in Table 1 (see "Materials and methods"). The collected data show that kinetic behavior of the proteins is not typical Michaelis–Menten behavior but, because the data fit better to the empirical Hill equation, is more consistent with a model with allosteric interactions within regulatory binding sites of the enzyme. These results agree with the kinetics observed for *Bacillus cereus* PIPLC (Bruce Birrel et al. 2003). Both purified proteins, LS-PIPLC and LS-PIPLC$_{\Delta CRY}$, showed similar kinetic behavior at 25 °C (Fig. 2, Table 1), demonstrating that the truncated protein is completely functional at this temperature.

Thermal stability of the enzymatic activity

The role of the βγ-crystallin domain in the thermal stability of the LS-PIPLC was initially evaluated by determining the residual activity of both proteins (LS-PIPLC and LS-PIPLC$_{\Delta CRY}$) after thermal inactivation. As it has been established that the binding of Ca^{2+} increases the stability of these domains, the calcium binding effect was evaluated by performing the assays in buffer containing 1 mM $CaCl_2$ or 1 mM EDTA. The purified enzymes were incubated at different temperatures (25, 50, and 60 °C) for 15 min prior to the enzymatic assay being conducted at 25 °C. Initial rates were determined in each case by using the fluorometric assay described earlier. Without Ca^{2+}, the full-length protein LS-PIPLC retained 85% of its initial activity after treatment at 50 °C, while LS-PIPLC$_{\Delta CRY}$ showed only 21% of its initial activity after the incubation. The two enzymes were almost completely inactivated after incubation at 60 °C (Table 2).

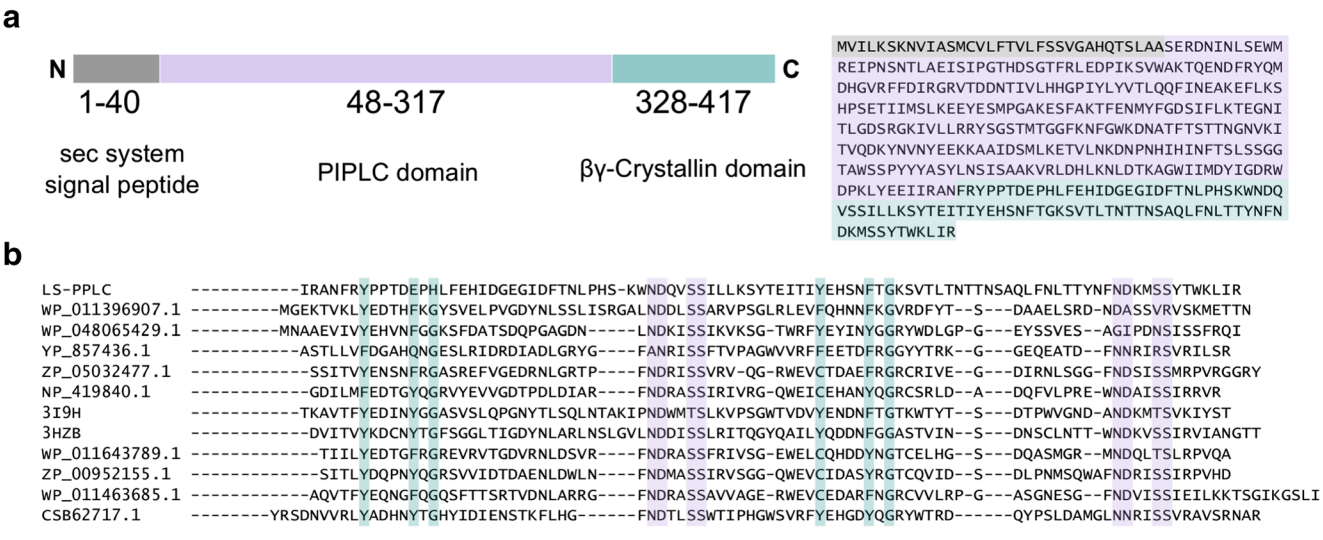

Fig. 1 LS-PIPLC is a new member of the βγ-crystallin superfamily. **a** LS-PIPLC showing the primary amino acid sequence of the protein and the arrangement of the different domains. **b** Multiple sequence analysis of LS-PIPLC with known βγ-crystallin domains. Conserved βγ-crystallin regions are highlighted in green (Y/FXXXXFXG) and purple (N/D-N/D-X-X-S/T-S/T). Only the βγ-crystallin domains of the respective sequences were selected and aligned by using ClustalW. Accession numbers are indicated

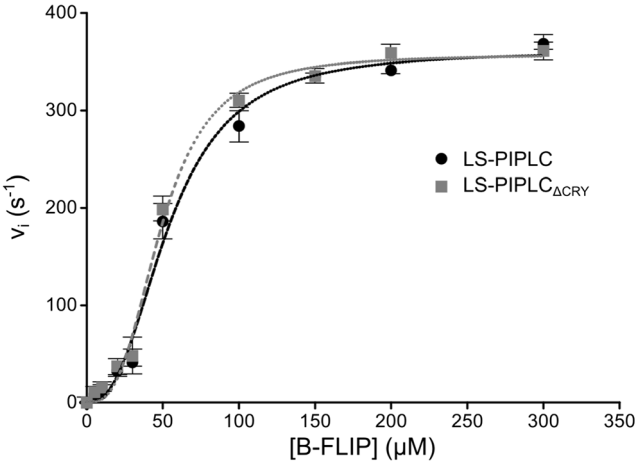

Fig. 2 Kinetics of LS-PIPLC and LS-PIPLC$_{\Delta CRY}$ with B-FLIP. Initial reaction rates as a function of substrate concentration for LS-PIPLC and LS-PIPLC$_{\Delta CRY}$. The dotted gray and black lines represent the fit to the empirical Hill equation for LS-PIPLC and LS-PIPLC$_{\Delta CRY}$, respectively. The data correspond to mean values of three independent experiments. Error bars correspond to the standard deviations

This experiment showed that the truncated protein is not as resistant to thermal denaturation as the full-length protein is, suggesting a stabilizing role for the βγ-crystallin domain. On the other hand, while Ca^{2+} had no effect on LS-PIPLC$_{\Delta CRY}$ stability, LS-PIPLC retained more than 99% of its initial activity at 50 °C and over 40% at 60 °C in the presence of Ca^{2+}, indicating a stabilizing role of Ca^{2+} binding (Table 2).

Effect of temperature and denaturing agents on LS-PIPLC stability

To further investigate the contribution of the βγ-crystallin domain to LS-PIPLC stability, the thermal denaturation of both proteins, LS-PIPLC and LS-PIPLC$_{\Delta CRY}$, was analyzed by using a thermal unfolding assay based on the use of a dye that emits fluorescence upon interaction with hydrophobic regions of the denatured protein. Fluorescence intensity was monitored after incubating the protein in the presence of SYPRO orange dye for 1 min at different temperatures between 25 and 90 °C. As shown in Fig. 3, there is a strong effect in protein stability exerted by the βγ-crystallin domain, as indicated by the difference of ~ 12 °C in Tm between LS-PIPLC (56.62 ± 0.27 °C) and LS-PIPLC$_{\Delta CRY}$ (44.65 ± 0.29 °C) analyzed in buffer containing EDTA. In addition, Ca^{2+} binding results in a further increase in the resistance to thermal denaturation of LS-PIPLC, given that the Tm

Table 1. Enzymatic parameters of LS-PIPLC and LS-PIPLC$_{\Delta CRY}$

	V_{hmax} (s^{-1})	K_h (mM)	*n*	R^2
LS-PIPLC	361.2 ± 13.3	53.8 ± 3.8	2.5 ± 0.4	0.99
LS-PIPLC$_{\Delta CRY}$	357.3 ± 9.5	48.7 ± 2.5	2.9 ± 0.4	0.99

Table 2. Residual activity

Temperature (ºC)	LS-PIPLC		LS-PIPLC$_{\Delta CRY}$	
	EDTA	$CaCl_2$	EDTA	$CaCl_2$
25	100 ± 0.7*	100 ± 4.9	100 ± 1.3	100 ± 3.9
50	85.3 ± 1.1	99.7± 6.7	21.8 ± 1.1	19.1 ± 1.4
60	5.3 ± 1.2	40.1 ± 6.4	0.8 ± 0.2	4.4 ± 0.7

*values expressed in percentage of initial activity at 25 ºC

increases by ~ 4 °C in the presence of Ca^{2+} (from 56.62 ± 0.27 to 60.34 ± 0.21 °C). In contrast, for LS-PIPLC$_{\Delta CRY}$, there is no difference in its thermal denaturation curves with and without the addition of Ca^{2+} (Table 3).

The effect of Ca^{2+} binding and the presence of the βγ-crystallin domain in LS-PIPLC stability were also assayed by measuring the fluorescence of tryptophan residues of the proteins in the presence of denaturing agents such as urea and guanidinium chloride (GdmCl). In globular proteins, the maximum of fluorescence emission from buried tryptophans is shifted to longer wavelengths upon exposure to solvent (Pace 1986). In this case, unfolding was monitored by using the ratio of 336/352-nm fluorescence intensities, with 336 and 352 nm being the respective fluorescence emission maxima of the folded and unfolded protein; normalized values were plotted (Fig. 4). As described above, the presence of the βγ-crystallin domain plays an important role in LS-PIPLC stability. In the absence of Ca^{2+}, LS-PIPLC and LS-PIPLC$_{\Delta CRY}$ presented a $[denaturant]_{1/2}$ (concentration at which the molar ratio of folded and unfolded protein is 1) of 2.4 and 2.0 M GdmCl and 4.9 and 2.8 M urea, respectively.

The stabilizing role of Ca^{2+} binding was also confirmed. The $[denaturant]_{1/2}$ of LS-PIPLC increased from 2.4 M GdmCl in the presence of EDTA to 3.3 M GdmCl with Ca^{2+}. This effect was also observed in urea, where the $[denaturant]_{1/2}$ shifted from 4.9 to 5.7 M (Table 3).

LS-PIPLC oil degumming at different temperatures

During industrial processing, crude oil is extracted from soybean at high temperatures and subsequently must be cooled to the temperature that is optimal for enzyme performance before oil degumming is conducted. After enzymatic treatment, the oil is heated to 85 °C in order to improve the efficiency of gum separation by centrifugation. Thermostable enzymes are therefore desirable for this process, and optimal temperatures close to 55–60 °C are preferred. Both enzymes, LS-PIPLC and LS-PIPLC$_{\Delta CRY}$, were assayed in laboratory-scale soybean oil degumming assays at 50 and 55 °C. For this purpose, 3 g of crude soybean oil was incubated at 50 °C with 10 μg of protein/g oil and PIPLC activity was followed indirectly by quantifying inorganic phosphate released, as previously

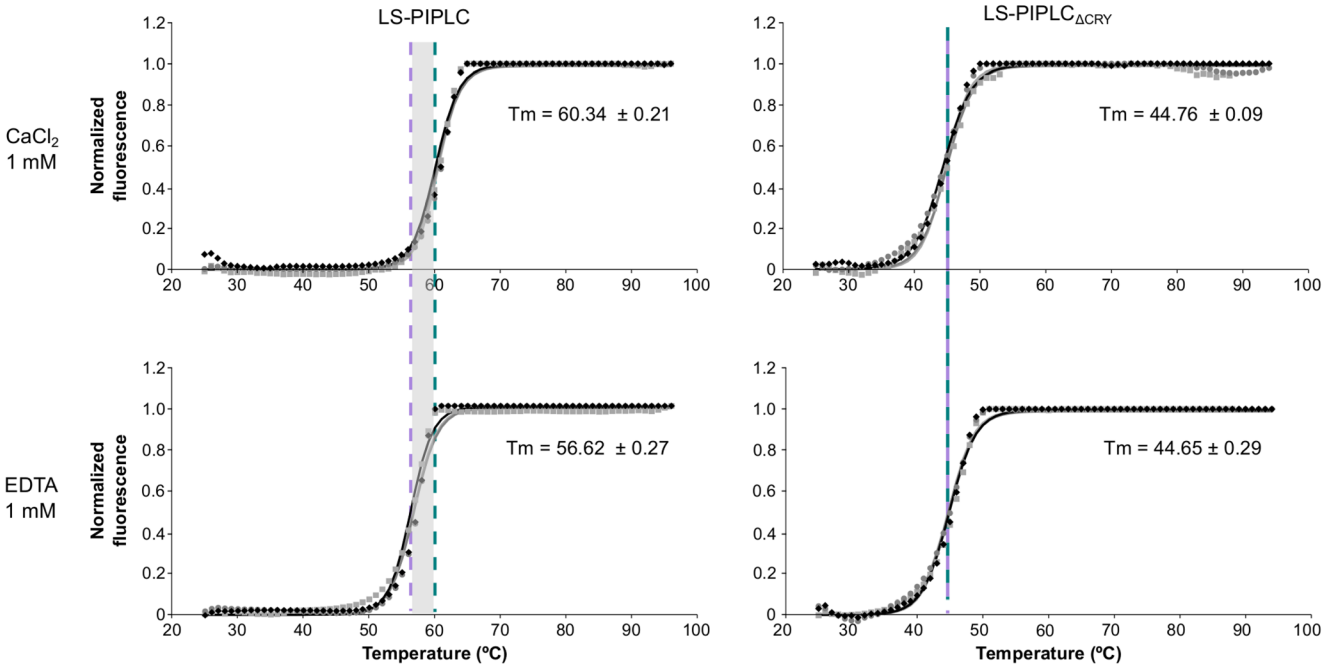

Fig. 3 LS-PIPLC and LS-PIPLC$_{\Delta CRY}$ thermal stability. Thermal shift analyses of LS-PIPLC and LS-PIPLC$_{\Delta CRY}$ in the presence of 1 mM $CaCl_2$ or 1 mM EDTA. The data correspond to three independent experiments. Estimated T_m's are indicated with a green dotted line for T_m estimated in the presence of $CaCl_2$ and with a purple dotted line for T_m estimated in the presence of EDTA. The gray zones symbolize the differences between the T_m with $CaCl_2$ or EDTA

described (Ravasi et al. 2015). The values obtained for phosphate correspond to the expected amount (6 mM) for complete hydrolysis of PI present in crude soybean oil (Cerminati et al. 2017), indicating that both enzymes were able to hydrolyze 100% of PI at 50 °C. Nonetheless, differences were observed at 55 °C. While LS-PIPLC hydrolyzed the totality of PI present in oil, LS-PIPLC$_{\Delta CRY}$ hydrolyzed only 50% of the PI, demonstrating that the βγ-crystallin domain plays an important role in stabilizing the entire protein under these conditions (Fig. 5a). In order to evaluate the effect of Ca^{2+} in LS-PIPLC stability in oil degumming, PI hydrolysis was evaluated at 50, 55, 60, 62, and 65 °C. As seen in Fig. 5b, the quantity of hydrolyzed PI remained nearly constant up to 60 °C either in the presence or in the absence of Ca^{2+}. At 62 °C in the presence of Ca^{2+}, LS-PIPLC hydrolyzed 85% of the PI compared to 50–55 °C, while in the absence of Ca^{2+}, the protein hydrolyzed only 40%. Even though at 65 °C LS-PIPLC is almost completely inactive, in the presence of Ca^{2+}, the hydrolysis was 10% of that shown at 50–55 °C, compared to 5% in the presence of the Ca^{2+} chelating agent EDTA.

Discussion

βγ-crystallin domains are ubiquitous in nature, having representatives in the three domains of life. The domains exist as single-domain proteins or part of multidomain proteins. However, little is known about the role of these domains in multidomain proteins because they have been studied mostly structurally as isolated domains (Mishra et al. 2014).

Here, LS-PIPLC is described as a member of the βγ-crystallin superfamily, and the role of this specific domain is analyzed. By deleting the βγ-crystallin domain from LS-PIPLC, it was shown that the domain has no effect in phospholipase activity at 25 °C. The wild-type and the mutated version of the protein, LS-PIPLC and LS-PIPLC$_{\Delta CRY}$, respectively, have very similar kinetic parameters when B-FLIP was used as a substrate (Table 1). This result also confirmed that the mutated version of the protein, LS-PIPLC$_{\Delta CRY}$, was able to fold properly and that the βγ-crystallin domain was not involved directly with the catalytic activity of the phospholipase. Since the βγ-crystallin domain does not appear to be

Table 3. Thermal and chemical denaturation parameters

	LS-PIPLC		LS-PIPLC$_{\Delta CRY}$	
	$CaCl_2$	EDTA	$CaCl_2$	EDTA
Tm (ºC)	60.34 ± 0.21	56.62 ± 0.27	44.76 ± 0.09	44.65 ± 0.29
[Denaturant]$_{1/2}$ urea (M)	3.3 ± 0.2	2.4 ± 0.3	2.1 ± 0.2	2.0 ± 0.1
[Denaturant]$_{1/2}$ GdmCl (M)	5.7 ± 0.2	4.9 ± 0.2	2.9 ± 0.1	2.8 ± 0.2

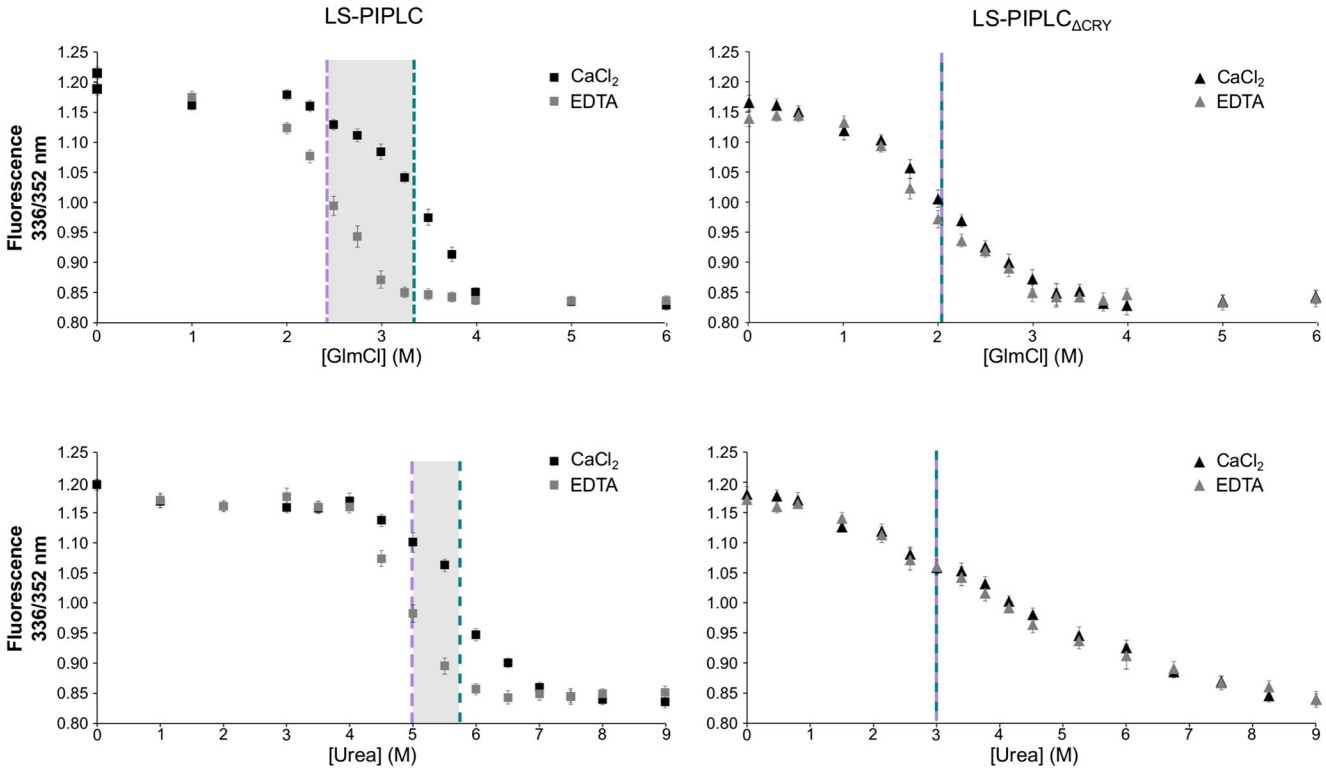

Fig. 4 Chemical stability of LS-PIPLC and LS-PIPLC$_{\Delta CRY}$. Normalized fluorescence of LS-PIPLC and LS-PIPLC$_{\Delta CRY}$ as a function of the concentration of urea or guanidinium chloride. The experiments were performed in the presence of 1 mM $CaCl_2$ or 1 mM EDTA. The data correspond to mean values of three independent experiments. Error bars correspond to the standard deviations. Estimated $[denaturant]_{1/2}$ is indicated with a green dotted line for $[denaturant]_{1/2}$ estimated in the presence of $CaCl_2$ and with a purple dotted line for $[denaturant]_{1/2}$ estimated in the presence of EDTA. The gray zones symbolize the differences between the $[denaturant]_{1/2}$ with $CaCl_2$ or EDTA

involved in the catalytic activity of the protein, its role was exploited by considering the known characteristics of the domain: high stability and Ca^{2+} binding.

In thermal and chemical-denaturing experiments, it was demonstrated that the βγ-crystallin domain exerts a stabilizing role in the entire protein, given that in the absence of the domain the protein was more labile (Figs. 3, 4, and 5).

It was further demonstrated that the presence of Ca^{2+} has a stabilizing role on LS-PIPLC, both in aqueous solution and in water-in-oil emulsion. However, this was not observed in the protein lacking the βγ-crystallin domain (LS-PIPLC$_{\Delta CRY}$). These observations are in agreement with published results that demonstrated a Ca^{2+}-induced gain in stability for microbial βγ-crystallin-isolated domains (Suman et al. 2011).

It is important to note that there were differences between the stabilities of the proteins observed in aqueous media and in the water-in-oil emulsion used for oil degumming (3% water in oil). LS-PIPLC$_{\Delta CRY}$ had a Tm of ~45 °C (either with EDTA or Ca^{2+}) and a residual activity of only 20% at 50 °C in aqueous buffer. However, the protein was able to completely hydrolyze PI in an oil degumming assay at 50 °C. In aqueous buffer, LS-PIPLC had a Tm of ~57 and ~60 °C in the presence of EDTA and Ca^{2+}, respectively (Fig. 4), but retained its activity at temperatures up to 60 and 62 °C in oil, while in the presence of EDTA and Ca^{2+}, respectively (Fig. 5).

It has been postulated that the conformational state of enzymes acting in interfaces is different from the one present in a water solution and that the interfacial lipid architecture might be considered an enzyme regulator (Berg et al. 2001). Because the substrate of the enzyme (phosphatidylinositol) is amphipathic, the catalytic event must occur at the oil-water interface. The presence of the phospholipase at the oil-water interface might have a stabilizing effect on the protein. Additionally, it has also been established for different enzymes that the presence of its substrate has an effect on their mechanical properties, making them kinetically more stable (Bippes et al. 2009; Zocher et al. 2012).

An in silico analysis of all sequenced bacterial βγ-crystallins, by using NCBI's Conserved Domain Database (Marchler-Bauer et al. 2017), shows that from 1808 sequences available, 51.6% (933) are single-domain proteins or have between two and seven repetitions of the βγ-crystallin domain with no other recognizable domains. The remaining 49.4% are associated with additional domains, distributed in 81 different architectures (Supplementary Table S1). It was observed that a high percentage (81.31%) of the bacterial proteins containing a βγ-crystallin domain is putative secreted

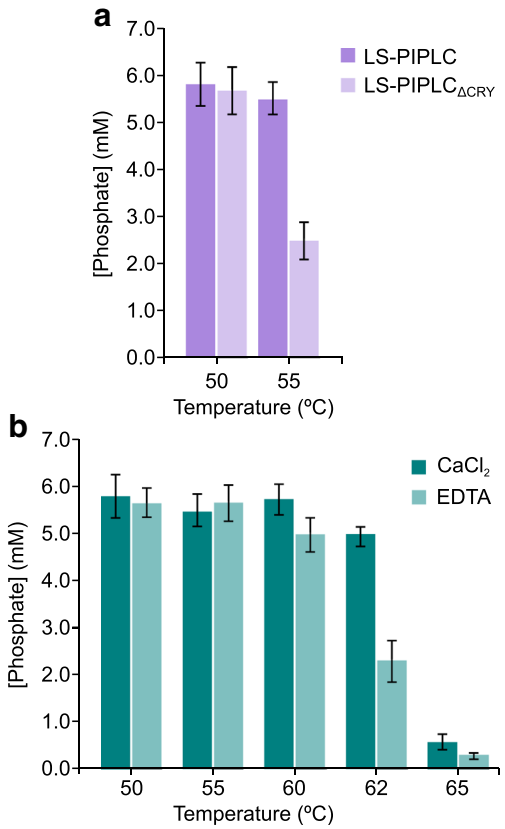

Fig. 5 Oil degumming with LS-PIPLC and LS-PIPLC$_{\Delta CRY}$. **a** Hydrolysis of PI by LS-PIPLC and LS-PIPLC$_{DCRY}$ was determined at 50 and 55 °C in crude soybean oil. **b** LS-PIPLC-mediated hydrolysis was determined at 50, 55, 60, 62, and 65 °C in the presence of 1 mM $CaCl_2$ or 1 mM EDTA. The data correspond to mean values of three independent experiments. Error bars correspond to the standard deviations

proteins, because they possess signal peptides for secretion [predicted by using Phobius (Käll et al. 2004)]. Given the well-documented high-stability properties of isolated βγ-crystallin domains and the high frequency of this domain in secreted proteins, it may be hypothesized that this domain represents a stability module recruited evolutionarily by many secreted bacterial proteins.

Protein structures in nature are built from a limited set of building blocks that are reused to create different proteins, from small single-domain proteins to large proteins comprising many domains (Levy 2017). In this work, it was shown that the deletion of the βγ-crystallin domain from LS-PIPLC does not alter the phospholipase catalytic properties of the enzyme, but that the thermal and chemical stability of the protein are markedly reduced. From a biotechnological point of view, it may be worth exploring the thermal stability of proteins containing this domain in combination with domains having potential industrial use, or adding this domain in order to artificially stabilize proteins.

Acknowledgements The authors wish to thank PLABEM for helping with the thermal shift assays and Luis Palacios and Ernesto Ventrici from Molinos Rio de la Plata and Hector Autino from Bunge Argentina for providing oil samples.

Funding information This work was funded by Agencia Nacional de Promoción Científica y Tecnológica PICT2014-0951 and PICT2015-0303.

Compliance with ethical standards

Conflict of interest The authors declare that they have no conflict of interest.

Ethical statement This article does not contain any studies with human participants or animals performed by any of the authors.

References

Aravind P, Mishra A, Suman SK, Jobby MK, Sankaranarayanan R, Sharma Y (2009a) The betagamma-crystallin superfamily contains a universal motif for binding calcium. Biochemistry 48:12180–12190. https://doi.org/10.1021/bi9017076

Aravind P, Suman SK, Mishra A, Sharma Y, Sankaranarayanan R (2009b) Three-dimensional domain swapping in nitrollin, a single-domain betagamma-crystallin from *Nitrosospira multiformis*, controls protein conformation and stability but not dimerization. J Mol Biol 385:163–177. https://doi.org/10.1016/j.jmb.2008.10.035

Berg OG, Gelb MH, Tsai M-D, Jain MK (2001) Interfacial enzymology: the secreted phospholipase A2-paradigm. Chem Rev 101:2613–2654. https://doi.org/10.1021/cr990139w

Bippes CA, Zeltina A, Casagrande F, Ratera M, Palacin M, Muller DJ, Fotiadis D (2009) Substrate binding tunes conformational flexibility and kinetic stability of an amino acid antiporter. J Biol Chem 284:18651–18663. https://doi.org/10.1074/jbc.M109.004267

Bloemendal H, de Jong W, Jaenicke R, Lubsen NH, Slingsby C, Tardieu A (2004) Ageing and vision: structure, stability and function of lens crystallins. Prog Biophys Mol Biol 86:407–485. https://doi.org/10.1016/j.pbiomolbio.2003.11.012

Bruce Birrel G, Zaikova TO, Rukavishnikov V, Keana JFW, Hayes Griffith O (2003) Allosteric interaction within subsites of a monomeric enzyme: kinetics of fluorogenic substrates of PI-specific phospholipase C. Biophys J 84(5):3264–3275. https://doi.org/10.1016/S0006-3495(03)70051-4

Castelli ME, Menzella H, Peirú S, Vetcher L (2016) Compositions and methods for oil degumming. PCT/US16/42844

Cerminati S, Eberhardt F, Elena CE, Peiru S, Castelli ME, Menzella HG (2017) Development of a highly efficient oil degumming process using a novel phosphatidylinositol-specific phospholipase C enzyme. Appl Microbiol Biotechnol 101:4471–4479. https://doi.org/10.1007/s00253-017-8201-0

Clout NJ, Kretschmar M, Jaenicke R, Slingsby C (2001) Crystal structure of the calcium-loaded spherulin 3a dimer sheds light on the evolution of the eye lens betagamma-crystallin domain fold. Structure 9:115–124

Dijkstra AJ (2011) Enzymatic degumming. Lipid Technol 23:36–38. https://doi.org/10.1002/lite.201100085

Erickson DR (1995) Chapter 10—degumming and lecithin processing and utilization. In: Practical handbook of soybean processing and utilization. AOCS Press, pp 174–183. doi:https://doi.org/10.1016/B978-0-935315-63-9.50014-0

Huynh K, Partch CL (2015) Current protocols in protein science: analysis of protein stability and ligand interactions by thermal shift assay.

Curr Protoc Protein Sci 79:28.29.21–28.29.14. https://doi.org/10.1002/0471140864.ps2809s79

Jaenicke R, Slingsby C (2001) Lens crystallins and their microbial homologs: structure, stability, and function. Crit Rev Biochem Mol Biol 36:435–499. https://doi.org/10.1080/20014091074237

Jobby MK, Sharma Y (2005) Calcium-binding crystallins from *Yersinia pestis*. Characterization of two single betagamma-crystallin domains of a putative exported protein. J Biol Chem 280:1209–1216. https://doi.org/10.1074/jbc.M409253200

Käll L, Krogh A, Sonnhammer ELL (2004) A combined transmembrane topology and signal peptide prediction method. J Mol Biol 338:1027–1036. https://doi.org/10.1016/j.jmb.2004.03.016

Kozlyuk N, Sengupta S, Bierma JC, Martin RW (2016) Calcium binding dramatically stabilizes an ancestral crystallin fold in tunicate betagamma-crystallin. Biochemistry 55:6961–6968. https://doi.org/10.1021/acs.biochem.6b00937

Levy Y (2017) Protein assembly and building blocks: beyond the limits of the LEGO brick metaphor. Biochemistry 56:5040–5048. https://doi.org/10.1021/acs.biochem.7b00666

Marchler-Bauer A, Bo Y, Han L, He J, Lanczycki CJ, Lu S, Chitsaz F, Derbyshire MK, Geer RC, Gonzales NR, Gwadz M, Hurwitz DI, Lu F, Marchler GH, Song JS, Thanki N, Wang Z, Yamashita RA, Zhang D, Zheng C, Geer LY, Bryant SH (2017) CDD/SPARCLE: functional classification of proteins via subfamily domain architectures. Nucleic Acids Res 45:D200–D203. https://doi.org/10.1093/nar/gkw1129

Mishra A, Krishnan B, Srivastava SS, Sharma Y (2014) Microbial betagamma-crystallins. Prog Biophys Mol Biol 115:42–51. https://doi.org/10.1016/j.pbiomolbio.2014.02.007

Pace CN (1986) Determination and analysis of urea and guanidine hydrochloride denaturation curves. Methods Enzymol 131:266–280

Pace CN, Laurents DV, Erickson RE (1992) Urea denaturation of barnase: pH dependence and characterization of the unfolded state. Biochemistry 31:2728–2734

Ravasi P, Braia M, Eberhardt F, Elena C, Cerminati S, Peiru S, Castelli ME, Menzella HG (2015) High-level production of *Bacillus cereus* phospholipase C in *Corynebacterium glutamicum*. J Biotechnol 216:142–148. https://doi.org/10.1016/j.jbiotec.2015.10.018

Sambrook J, Fritsch EF, Maniatis T (1989) Molecular cloning : a laboratory manual. Cold Spring Harbor Laboratory, Cold Spring Harbor

Santoro MM, Bolen DW (1988) Unfolding free energy changes determined by the linear extrapolation method. 1. Unfolding of phenylmethanesulfonyl alpha-chymotrypsin using different denaturants. Biochemistry 27:8063–8068

Srivastava SS, Jamkhindikar AA, Raman R, Jobby MK, Chadalawada S, Sankaranarayanan R, Sharma Y (2017) A transition metal-binding, trimeric betagamma-crystallin from methane-producing Thermophilic Archaea, *Methanosaeta thermophila*. Biochemistry 56:1299–1310. https://doi.org/10.1021/acs.biochem.6b00985

Srivastava SS, Mishra A, Krishnan B, Sharma Y (2014) Ca^{2+}–binding motif of βγ-crystallins. J Biol Chem 289:10958–10966

Studier FW, Rosenberg AH, Dunn JJ, Dubendorff JW (1990) Use of T7 RNA polymerase to direct expression of cloned genes. Methods Enzymol 185:60–89

Suman SK, Mishra A, Ravindra D, Yeramala L, Sharma Y (2011) Evolutionary remodeling of betagamma-crystallins for domain stability at cost of Ca^{2+} binding. J Biol Chem 286:43891–43901. https://doi.org/10.1074/jbc.M111.247890

Suman SK, Ravindra D, Sharma Y, Mishra A (2013) Association properties and unfolding of a betagamma-crystallin domain of a Vibrio-specific protein. PLoS One 8:e53610. https://doi.org/10.1371/journal.pone.0053610

Sumner JB (1944) A method for the colorimetric determination of phosphorus. Science 100:413–414. https://doi.org/10.1126/science.100.2601.413

Teintze M, Inouye M, Inouye S (1988) Characterization of calcium-binding sites in development-specific protein S of *Myxococcus xanthus* using site-specific mutagenesis. J Biol Chem 263:1199–1203

Vendra VP, Khan I, Chandani S, Muniyandi A, Balasubramanian D (2016) Gamma crystallins of the human eye lens. Biochim Biophys Acta 1860:333–343. https://doi.org/10.1016/j.bbagen.2015.06.007

Wedler FC (1976) Enzyme kinetics: behavior and analysis of rapid equilibrium and steady-state enzyme systems. Author: Irwin H. Segal (University of California, Davis). Published by Wiley-Interscience, New York, 1975. Price: $24.50. No. of pages: 957. In J Chem Kinet 8:159–159. https://doi.org/10.1002/kin.550080117

Zocher M, Zhang C, Rasmussen SG, Kobilka BK, Muller DJ (2012) Cholesterol increases kinetic, energetic, and mechanical stability of the human beta2-adrenergic receptor. Proc Natl Acad Sci U S A 109:E3463–E3472. https://doi.org/10.1073/pnas.1210373109